Tooth-shaped plasmonic waveguide filters with nanometeric sizes

Xian-Shi Lin and Xu-Guang Huang*

Laboratory of Photonic Information Technology, South China Normal University, Guangzhou, 510006, China
**Corresponding author: huangxg@scnu.edu.cn*

Received August 1, 2008; revised October 13, 2008; accepted October 16, 2008;
posted October 28, 2008 (Doc. ID 99693); published November 26, 2008

A novel nanometeric plasmonic filter in a tooth-shaped metal-insulator-metal waveguide is proposed and demonstrated numerically. An analytic model based on the scattering matrix method is given. The result reveals that the single tooth-shaped filter has a wavelength-filtering characteristic and an ultracompact size in the length of a few hundred nanometers, compared to gratinglike surface plasmon polariton (SPP) filters. Both analytic and simulation results show that the wavelength of the trough of the transmission has linear and nonlinear relationships with the tooth depth and the tooth width, respectively. The waveguide filter could be utilized to develop ultracompact photonic filters for high integration. © 2008 Optical Society of America

OCIS codes: 130.3120, 230.7408, 240.6680, 290.5825.

Surface plasmons are waves that propagate along a metal–dielectric interface with an exponentially decaying field in both sides [1,2]. The unique properties of surface plasmon polaritons (SPPs) have shown the potential to overcome the diffraction limit in conventional optics, which could be utilized to achieve nanoscale photonic devices for high integration. Several different metal–insulator–metal (MIM) waveguide structures based on SPPs have been numerically and/or experimentally demonstrated, such as U-shaped waveguides [3], splitters [4], Y-shaped combiners [5], multimode-interferometers [6], couplers [7,8], Mach–Zehnder interferometers [9,10], Bragg mirrors [11], and photonic bandgap structures [12]. To achieve wavelength-filtering characteristics, SPP Bragg reflectors and nanocavities have been proposed. They include the metal heterostructures constructed with several periodic slots placed vertically along an MIM waveguide [13,14], the Bragg grating fabricated by periodically modulating the thickness of thin metal stripes embedded in an insulator [15], and the periodic structure formed by changing alternately two kinds of the insulators with the same width [16] or different widths [17,18]. Recently, a high-order plasmonic Bragg reflector with a periodic modulation of the core index of the insulators [19] and a structure with a periodic variation of the width of the insulator in an MIM waveguide [20] have been proposed. Most of the structures mentioned above, however, have the period number of $N>9$ with the total lengths over 4 μm and beyond the subwavelength scale, which result in a relatively high insertion loss of several decibels. In this Letter, a nanoscale SPP filter based on the MIM waveguide consisting of a single rectangular tooth is proposed. The SPP distributions and propagations are characterized by the method of finite-difference time domain (FDTD), with perfect-matching-layer absorbing boundary conditions. An analytic model based on the scattering matrix method is derived to explain the filtering mechanism of the structure.

To begin with the dispersion relation of the fundamental TM mode in an MIM waveguide (shown in the inset of Fig. 1) is given by [15,21]

$$\varepsilon_{\text{in}} k_{z2} + \varepsilon_m k_{z1} \coth\left(-\frac{ik_{z1}}{2} w\right) = 0 \tag{1}$$

with k_{z1} and k_{z2} defined by momentum conservations

$$k_{z1}^2 = \varepsilon_{\text{in}} k_0^2 - \beta^2, \quad k_{z2}^2 = \varepsilon_m k_0^2 - \beta^2, \tag{2}$$

where ε_{in} and ε_m are, respectively, dielectric constants of the insulator and the metal and $k_0 = 2\pi/\lambda_0$ is the free-space wave vector. The propagation constant β is represented as the effective index $n_{\text{eff}} = \beta/k_0$ of the waveguide for SPPs. The real part of n_{eff} of the slit waveguide as a function of the slit width at different wavelengths is shown in Fig. 1. It should be noted that the dependence of n_{eff} on the waveguide width is also suitable to the small part or region of the tooth waveguide with the tooth width of w_t shown in Fig. 2. The imaginary part of n_{eff} refers to the propagation length that is defined as the length over which the power carried by the wave decays to $1/e$ of its initial value: $L_{\text{spps}} = \lambda_0/[4\pi \cdot \text{Im}(n_{\text{eff}})]$. In the calcu-

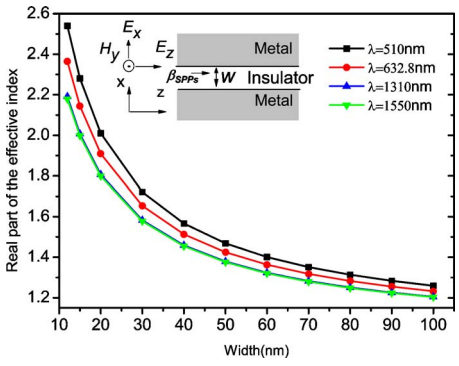

Fig. 1. (Color online) Real part of the effective index of refraction versus the width of a MIM slit waveguide structure.

0146-9592/08/232874-3/$15.00

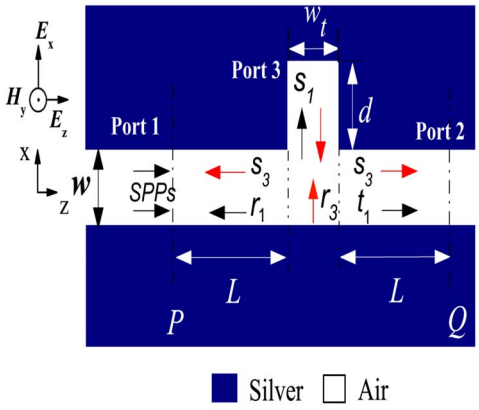

Fig. 2. (Color online) Structure schematics of a single tooth-shaped waveguide filter with a slit width of w, a tooth width of w_t, and a tooth depth of d.

lation above and the following simulations, the insulator in all of the structures is assumed to be air ($\varepsilon_{in}=1$), and the frequency-dependent complex relative permittivity of silver is characterized by the Drude model $\varepsilon_m(\omega)=\varepsilon_\infty-\omega_p^2/\omega(\omega+i\gamma)$. Here $\omega_p=1.38\times10^{16}$ Hz is the bulk plasma frequency, which represents the natural frequency of the oscillations of free conduction electrons; $\gamma=2.73\times10^{13}$ Hz is the damping frequency of the oscillations, ω is the angular frequency of the incident electromagnetic radiation, and ε_∞ stands for the dielectric constant at infinite angular frequency with a value of 3.7 [20].

The tooth-shaped waveguide filter is shown in Fig. 2. In the following FDTD simulations, the grid sizes in the x and the z directions are chosen to be 5 nm $\times$5 nm. The fundamental TM mode of the plasmonic waveguide is excited by a dipole source. Two power monitors are, respectively, set at the points of P and Q to detect the incident and the transmission fields for calculating the incident power of P_{in} and the transmitted power of P_{out}. The transmittance is defined to be $T=P_{out}/P_{in}$. The length of L is fixed to be 300 nm while the tooth width and depth are, respectively, $w_t=50$ and $d=100$ nm. The tabulation of the optical constants of silver [22] is used in the simulation. As shown in Fig. 3(a), the tooth-shaped waveguide is of a filtering function; a trough occurs at the free-space wavelength at nearly 784 nm with the transmittance of ~0%. The maximum transmittance at the wavelengths longer than 1700 nm is over 90%. The contour profiles of the field distributions around the tooth-shaped area at different wavelengths are shown in Figs. 3(b)–3(d). The filtering structure is distinguished from the Bragg reflectors based on a periodical heterostructure.

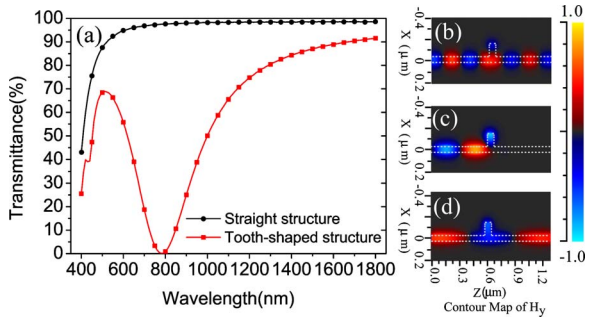

Fig. 3. (Color online) (a) Transmission of the single tooth-shaped MIM waveguide compared with a straight MIM slit waveguide. The width of the waveguide is $w=50$ nm, and the tooth width and depth are, respectively, $w_t=50$ and $d=100$ nm. The contour profiles of field H_y of the tooth-shaped waveguide at different wavelengths of (b) $\lambda=510$, (c) $\lambda=783$, and (d) $\lambda=1550$ nm.

The phenomenon above can be physically explained in the scattering matrix theory [23] as follows:

$$\begin{pmatrix} E_1^{out} \\ E_2^{out} \\ E_3^{out} \end{pmatrix} = S \begin{pmatrix} E_1^{in} \\ E_2^{in} \\ E_3^{in} \end{pmatrix}, \tag{3}$$

where

$$S = \begin{bmatrix} r_1 & t_1 & s_3 \\ t_1 & r_1 & s_3 \\ s_1 & s_1 & r_3 \end{bmatrix},$$

r_i, t_i, and s_i ($i=1,2,3$) are, respectively, the reflection, transmission, and splitting coefficients of an incident beam from Port i ($i=1,2,3$) caused by the structure; and E_i^{in} and E_i^{out} stand for the fields of incident and output beams at Port i, respectively. Using the fact that $|S|=1$, one can obtain

$$r_1^2 r_3 + 2t_1 s_1 s_3 - 2r_1 s_1 s_3 - t_1^2 r_3 = 1. \tag{4}$$

For the case of $E_2^{in}=0$, one has

$$E_2^{out} = t_1 E_1^{in} + s_3 E_3^{in}, \tag{5}$$

in which E_3^{in} is given as follows:

$$\begin{aligned} E_3^{in} &= s_1 E_1^{in} \exp(i\phi(\lambda))(1 + r_3 \exp(i\phi(\lambda)) \\ &\quad + r_3^2 \exp(2i\phi(\lambda)) + \dots) \\ &= \frac{s_1 E_1^{in}}{1 - r_3 \exp(i\phi(\lambda))} \exp(i\phi(\lambda)), \end{aligned} \tag{6}$$

where the phase delay $\phi(\lambda)=(4\pi/\lambda)n_{eff}\cdot d+\Delta\varphi(\lambda)$ and $\Delta\varphi(\lambda)$ is the phase shift caused by the reflection on the air-silver surface. Combining Eqs. (5) and (6), the output field at Port 2 is derived as

$$E_2^{out} = t_1 E_1^{in} + \frac{s_1 s_3 E_1^{in}}{1 - r_3 \exp(i\phi(\lambda))} \exp(i\phi(\lambda)). \tag{7}$$

Therefore, the transmittance T from Port 1 to Port 2 is given by

$$T = \left| \frac{E_2^{out}}{E_1^{in}} \right|^2 = \left| t_1 + \frac{s_1 s_3}{1 - r_3 \exp(i\phi(\lambda))} \exp(i\phi(\lambda)) \right|^2. \tag{8}$$

It can be seen from Eq. (8) that, if the phase satisfies $\phi(\lambda)=(2m+1)\pi$ ($m=0,1,2,\dots$), the two terms inside the absolute value sign on the right of the equation will cancel each other [as can be seen in Fig. 3(c)] so that the transmittance T will become minimum.

Therefore, the wavelength λ_m of the trough of transmission is determined as follows:

$$\lambda_m = \frac{4n_{\text{eff}}d}{(2m+1) - \dfrac{\Delta\varphi(\lambda)}{\pi}}. \quad (9)$$

It can be seen that the wavelength λ_m is linear to the tooth depth d and depends on tooth width w_t through the somewhat inverse-proportionlike relationship between n_{eff} and w_t shown in Fig. 1.

Figure 4(a) shows the transmission spectra of the waveguide filters with various tooth widths of w_t. The maximum transmittance can reach 97%. Figure 4(b) shows the wavelength of the trough versus the tooth width of w_t. The primary trough of the transmission moves very significantly to the short wavelength (blueshift) with an increase of w_t for $w_t < 20$ nm. The shift rate rapidly becomes small after $w_t > 20$ nm and tends to be saturated when $w_t > 200$ nm. As revealed in Eq. (9), the above relationship between the trough position and w_t mainly results from the contribution of the inverse-proportionlike dependence of n_{eff} on w_t. The change rate of $\Delta n_{\text{eff}}/\Delta w_t$ within the tooth width of 20 nm is much higher than that of $\Delta n_{\text{eff}}/\Delta w_t$ after $w_t > 20$ nm, as shown in Fig. 1 and [13], and finally becomes saturated after $w_t > 200$ nm. Obviously, tooth width w_t should be chosen within the range of 20–200 nm to avoid the critical behavior and the difficulty in the fabrication process.

Figure 5(a) shows the transmission spectra of the filters with different tooth depths of d. It is found that the wavelength of the trough shifts to a long wavelength with an increase of d. Figure 5(b) reveals that the wavelength of the trough has a linear relationship with the tooth depth as our expectation in Eq. (9). Therefore, one can realize the filter function in various required wavelengths with high performance by changing the width and/or the depth of the tooth. For example, to obtain a filter with a trough at a wavelength of 1550 nm, the structural parameters of $w_t = w = 50$ nm and $d = 237.5$ nm can be chosen.

In summary, a novel plasmonic MIM waveguide filter with a single tooth is investigated. The filter is of an ultracompact size with hundreds of nanometers in length and low insertion loss. It is promised to reduce fabrication difficulties, compared with previous gratinglike heterostructures with micrometers in length. Our results suggest that the new structure could be utilized to develop plasmonic filters on metallic surfaces with extreme high integration for planar nanophotonic circuits.

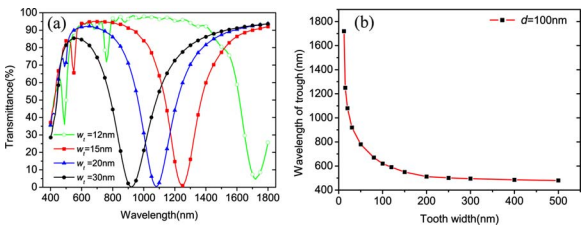

Fig. 4. (Color online) (a) Transmission spectra of the waveguide filters with various tooth widths of w_t at a fixed tooth depth of $d = 100$ nm and a slit width of $w = 50$ nm. (b) Wavelength of the trough versus the tooth width of w_t.

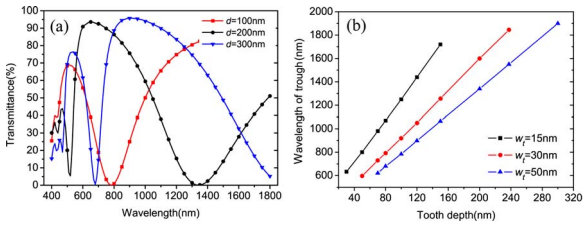

Fig. 5. (Color online) (a) Transmission spectra of the waveguide filters with different tooth depths of d and with a given tooth width of $w_t = 50$ nm and a slit width of $w = 50$ nm. (b) Wavelength of the trough versus the tooth depth of d with $w_t = 15$, $w_t = 30$, and $w_t = 50$ nm.

The authors acknowledge the financial support from the Natural Science Foundation (NSF) of Guangdong Province, China (grant 07117866).

References

1. H. Raether, *Surface Plasmon on Smooth and Rough Surfaces and on Gratings* (Springer-Verlag, 1988).
2. W. L. Barnes, A. Dereux, and T. Ebbesen, Nature **424**, 824 (2003).
3. T. Lee and S. Gray, Opt. Express **13**, 9652 (2005).
4. G. Veronis and S. Fan, Appl. Phys. Lett. **87**, 131102 (2005).
5. H. Gao, H. Shi, C. Wang, C. Du, X. Luo, Q. Deng, Y. Lv, X. Lin, and H. Yao, Opt. Express **13**, 10795 (2005).
6. Z. Han and S. He, Opt. Commun. **278**, 199 (2007).
7. T. Nikolajsen, K. Leosson, and S. I. Bozhevolnyia, Appl. Phys. Lett. **85**, 5833 (2004).
8. H. Zhao, X. Huang, and J. Huang, Phys. E **40**, 3025 (2008).
9. B. Wang and G. Wang, Opt. Lett. **29**, 1992 (2004).
10. Z. Han, L. Liu, and E. Forsberg, Opt. Commun. **259**, 690 (2006).
11. H. Ditlbacher, J. R. Krenn, G. Schider, A. Leitner, and F. R. Aussenegg, Appl. Phys. Lett. **81**, 1762 (2002).
12. S. I. Bozhevolnyi, J. E. Erland, K. Leosson, P. M. W. Skovgaard, and J. M. Hvam, Phys. Rev. Lett. **86**, 3008 (2001).
13. B. Wang and G. Wang, Appl. Phys. Lett. **87**, 013107 (2005).
14. W. Lin and G. Wang, Appl. Phys. Lett. **91**, 143121 (2007).
15. A. Boltasseva, S. I. Bozhevolnyi, T. Nikolajsen, and K. Leosson, J. Lightwave Technol. **24**, 912 (2006).
16. A. Hossieni and Y. Massoud, Opt. Express **14**, 11318 (2006).
17. A. Hosseini, H. Nejati, and Y. Massoud, Opt. Express **16**, 1475 (2008).
18. J. Q. Liu, L. L. Wang, M. D. He, W. Q. Huang, D. Y. Wang, B. S. Zou, and S. C. Wen, Opt. Express **16**, 4888 (2008).
19. J. Park, H. Kim, and B. Lee, Opt. Express **16**, 413 (2008).
20. Z. Han, E. Forsberg, and S. He, IEEE Photon. Technol. Lett. **19**, 91 (2007).
21. J. A. Dionne, L. A. Sweatlock, and H. A. Atwater, Phys. Rev. B **73**, 035407 (2006).
22. E. D. Palik, *Handbook of Optical Constants of Solids* (Academic, 1985).
23. H. A. Haus, *Waves and Fields in Optoelectronics* (Prentice-Hall, 1984).